Published in final edited form as:

Adv Healthc Mater. 2015 December 9; 4(17): 2677–2687. doi:10.1002/adhm.201500618.

Injectable, Pore-Forming Hydrogels for *In Vivo* Enrichment of Immature Dendritic Cells

Dr. C. S. Verbeke,

Wyss Institute for Biologically Inspired Engineering, Harvard University, Boston, MA 02115, USA

D. J. Mooney [Prof.], and

Wyss Institute for Biologically Inspired Engineering, Harvard University, Boston, MA 02115, USA

John A. Paulson

School of Engineering and Applied Sciences, Harvard University, Cambridge, MA 02138, USA

D. J. Mooney: mooneyd@seas.harvard.edu

Abstract

Biomaterials-based vaccines have emerged as a powerful method to evoke potent immune responses directly *in vivo*, without the need for *ex vivo* cell manipulation, and modulating dendritic cell (DC) responses in a non-inflammatory context could enable the development of tolerogenic vaccines to treat autoimmunity. This study describes the development of a non-inflammatory, injectable hydrogel system to locally enrich DCs *in vivo* without inducing their maturation or activation, as a first step towards this goal. Alginate hydrogels that form pores *in situ* were characterized and used as a physical scaffold for cell infiltration. These gels were also adapted to control the release of GM-CSF, a potent inducer of DC recruitment and proliferation. *In vivo*, sustained release of GM-CSF from the pore-forming gels led to the accumulation of millions of cells in the material. These cells were highly enriched in $CD11b^+$ $CD11c^+$ DCs, and further analysis of cell surface marker expression indicated these DCs were immature. This study demonstrates that a polymeric delivery system can mediate the accumulation of a high number and percentage of immature DCs, and may provide the basis for further development of materials-based, therapeutic vaccines.

Keywords

immunotherapy; hydrogels; dendritic cells; alginate; gold nanoparticles

Introduction

Numerous vaccines have had a tremendous positive impact on global human health. However, traditional approaches to vaccination have had limited success when applied to a number of diseases, and there exists a need for innovative vaccine technologies. In

Correspondence to: D. J. Mooney, mooneyd@seas.harvard.edu.

Supporting Information

Supporting Information is available from the Wiley Online Library or from the author.

particular, the development of a tolerogenic vaccine that prevents the immune system from carrying out aberrant, destructive responses against harmless antigens would be transformative for the treatment of autoimmune diseases, allergies, and transplant rejection. Dendritic cells (DCs) act as the sentinels of the immune system and orchestrate adaptive immune responses, which are carried out by T and B cells. In addition to mounting inflammatory responses against pathogens, DCs also play a critical and active role in maintaining peripheral tolerance.[1–4] The mechanisms that control DC responses upon encounter of an antigen are complex; DCs integrate both soluble (danger signals, cytokines, growth factors) and insoluble (cell surface receptors, extracellular matrix) cues that they encounter in the local micro environment. In order to translate a growing mechanistic understanding of DC biology into effective *in vivo* therapies, tools will be required to present DCs with appropriate cues that allow precise control over their behavior.

Biomaterials-based vaccines are a promising new class of technologies that can modulate immune responses in ways that have not been possible previously using immunomodulatory small molecule or antibody drugs. Biomaterials can be used to control cell behavior directly *in vivo*, without the need for costly and complex *ex vivo* cell manipulation, which represents a significant advantage over cell therapies. One approach to using biomaterials for immunomodulation is to target DCs or other immune cells *in vivo* using nanoparticles.[5,6] Another promising strategy involves using porous material scaffolds that immune cells can infiltrate in order to provide a site where the cells can be programmed by well-defined, localized cues.[7] Using a scaffold to enrich and program immune cells in a localized manner is appealing for inducing antigen-specific tolerance, since systemic delivery of a disease-related antigen could re-activate pathogenic effector T cells and exacerbate disease.[8] However, the same material systems used to create potent cancer vaccines[7] may not be appropriate for inducing tolerance, since the inherent inflammatory properties of materials such as PLGA[9,10] and the need for surgical implantation may cause inflammation and inhibit tolerogenic responses. A new material platform that is inherently non-inflammatory and can be delivered in a minimally invasive manner would expand the utility of materials-based vaccines and likely make them more amenable for inducing tolerance.

A number of biocompatible injectable hydrogel systems have been developed for drug delivery and tissue engineering applications using a variety of different materials.[11–13] One such biomaterial, alginate, is a highly biocompatible, non-inflammatory polysaccharide that is categorized by the FDA as a GRAS (Generally Recognized As Safe) food ingredient and is FDA-approved for use as an excipient, a wound dressing material,[14] and as part of a few medical products that are placed within the body. The physical and chemical properties of alginate gels are highly tunable, allowing control over characteristics such as stiffness, degradation, and cell adhesion.[15] Although standard alginate hydrogels are nanoporous and do not allow cell infiltration or migration, several different techniques have been developed for fabricating alginate gels that contain macro-scale pores[16–18] and can be delivered in a minimally invasive manner through a needle.[17,18] In particular, ionically crosslinked pore-forming alginate gels result from the incorporation of rapidly degrading porogen beads into a bulk gel, such that the degradation of the porogens leads to the formation of pores *in situ*.[18] These pore-forming gels are permissive for cell migration and have been used as a

cell delivery platform to disperse cells after implantation.[18] Here, this material system was adapted to mediate local enrichment of DCs within the gels *in vivo*.

Since non-inflammatory materials would not be expected to activate the immune system or induce cell infiltration on their own, a bioactive factor would be needed to selectively enrich DCs within the material. Granulocyte-macrophage colony stimulating factor (GM-CSF) is a small (14.2 kDa in mouse, 14.6 kDa in human) single-chain glycoprotein that is a potent inducer of DC differentiation, proliferation, and migration. GM-CSF is commonly used as a media supplement to differentiate myeloid precursors from bone marrow or peripheral blood into DCs, which remain immature in the absence of other inflammatory cytokines or TLR ligands.[19] GM-CSF has also been shown to induce chemotaxis and chemokinesis of DCs *in vitro*.[20] Although GM-CSF is used in cell-based cancer vaccines,[21] it can have contradictory effects, ranging from enhancing immune responses to inducing suppressive or toloregenic effects,[22] depending on the dose and context in which it is administered. In the setting of autoimmune diseases, several reports have demonstrated that administration of GM-CSF can have tolerizing effects and delay disease in mouse models of type 1 diabetes[23,24] or experimental autoimmune myasthenia gravis (EAMG).[25] In particular, these studies observed that GM-CSF treated DCs led to an increase in regulatory T cells *in vitro*[26] and *in vivo*.[23]

Here, we describe a non-inflammatory material system that can be administered in a minimally invasive manner to locally enrich immature DCs *in vivo*. Pore-forming macroporous alginate hydrogels were used as a physical support for cell infiltration and also as a delivery system for the cytokine GM-CSF. Effective accumulation of a highly enriched population of DCs was achieved by controlling the release kinetics of GM-CSF from alginate hydrogels, as well as the pore structure of the gels. When administered *in vivo*, this system led to the accumulation of several million DCs, which were characterized and found to exhibit a phenotype consistent with immature or non-inflammatory DCs.

Results

Characterization of Pore-Forming Alginate Hydrogels

Pore-forming alginate hydrogels were fabricated by incorporating rapidly degrading porogen beads into a non-degrading bulk gel. Porogens were composed of alginate that was chemically modified to accelerate its degradation, then pre-crosslinked to create beads that remained intact even after mixing and crosslinking of the bulk gel (Figure 1A). To select an optimal porogen formulation, the degradation kinetics at 37°C were determined for different formulations (Figure 1B). 2% w/v alginate hydrogels made from 7.5% oxidized/reduced alginate degraded almost completely in only 3 days. In contrast, unmodified alginate gels showed a small initial reduction in dry mass, which was likely due to the diffusion of sulfate ions and unbound calcium ions following crosslinking, but the dry mass then plateaued and remained stable over time, indicating that the gels did not degrade. Binary mixtures of 7.5% oxidized/reduced alginate with a small amount of unmodified alginate exhibited intermediate degradation profiles. Varying the composition of the polymer and other fabrication parameters, such as the coaxial airflow rate, allowed control over not only the degradation rate, but also the size of the porogen beads (Supporting Figure S1). For

subsequent work, a combination of 2% w/v oxidized/reduced alginate together with 0.25% w/v unmodified alginate was used to fabricate porogens that exhibited a mean diameter of 230 μm. This formulation was selected because it displayed sufficient mechanical stability to withstand the porogen bead fabrication process, yet still degraded rapidly, exhibiting 70% degradation in 5 days. When gels containing these porogens were incubated at 37°C *in vitro*, their interconnected porosity was significantly higher than that of nanoporous gels, indicating that the porogens degraded and formed voids within the bulk gel (Figure 1C). Consistent with this finding, gels containing FITC-labeled porogens exhibited a loss of FITC signal from the gels (Supporting Figure S2A) and a concomitant release of FITC into the media (Supporting Figure S2B) as the porogens degraded over time at 37°C. The pore-forming gels were subsequently used as the basis for the material system to recruit DCs *in vivo*.

Tunable Release of the Cytokine GM-CSF from Alginate Hydrogels

To achieve effective DC accumulation, the material system was engineered for sustained release of the cytokine GM-CSF. Different methods for incorporating the protein into the hydrogels were used to obtain different release profiles. Direct incorporation of GM-CSF into 2% w/v alginate hydrogels led to a rapid burst release when the gels were incubated at 37°C. Over 95% of the encapsulated protein was released within the first 24 h, followed by a greatly reduced release rate over the next few days (Figure 2A). By 1 week, over 98% of the GM-CSF was released (Figure 2A). To achieve amore sustained release profile, GM-CSF was coupled to gold nanoparticles (AuNPs) via formation of covalent bonds between the gold and the thiol groups on cysteine residues in GM-CSF, prior to incorporation in the gels. The AuNPs used for this study measured approximately 13 nm in diameter and were monodisperse, with a polydispersity index (PDI) < 0.05 (Supporting Figure S3A). Immediately after conjugation of 3ug of GM-CSF to AuNPs, 2ug of GM-CSF could be recovered from the particles, while only 44ng of free GM-CSF were detected in the supernatant (Supporting Figure S3B). When GM-CSF-conjugated AuNPs were incubated in HBSS (Hank's Balanced Salt Solution) at 37°C, approximately50% of the bound GM-CSF was released from the particles in the first day, and release continued at a sustained rate over 4 weeks, at which point 98% of the GM-CSF was released (Figure 2B). At the end of these release studies, which were conducted over 4 weeks at 37°C, greater than 75% of the GM-CSF initially bound was recovered (Supporting Figure S3C). Importantly, GM-CSF remained bioactive following release from AuNPs (Supporting Figure S4).

When AuNPs coated with GM-CSF were incorporated into alginate gels (Figure 2C), it became apparent that the media used to formulate the gels affected the rate of GM-CSF release. GM-CSF dissociated rapidly from AuNPs in the presence of cystine, exhibiting almost 98% release by 24 h (Supporting Figure S5A). In contrast, the retention of GM-CSF on AuNPs was significantly higher in cystine-free media (Supporting Figure S5B). In light of these findings, GM-CSF-conjugated AuNPs were incorporated into alginate hydrogels, and the profiles of GM-CSF release were compared between gels formulated with and without cystine (Figure 2D). When gels were fabricated using standard media containing cystine, the release of GM-CSF was rapid (Figure 2D) and almost identical to the release of free GM-CSF incorporated directly into gels (Figure 2A). On the other hand, gels

formulated without cystine released GM-CSF in a sustained manner over several weeks (Figure 2D), exhibiting a release profile that was similar to the release of GM-CSF from AuNPs alone (Figure 2B).

Influence of GM-CSF Release Kinetics and Gel Porosity on Cell Infiltration *In Vivo*

In order to examine cell infiltration *in vivo*, pore-forming gels were injected subcutaneously into the flanks of mice. Blank gels were compared to gels designed to release GM-CSF either rapidly (free GM-CSF) or in a sustained manner (GM-CSF conjugated to AuNPs). To test whether the AuNPs themselves exerted any effects independently of GM-CSF, AuNPs were also conjugated to a control protein, consisting of Fab fragments from mouse IgG, which are not expected to elicit any biological activity. Gels that did not contain any GM-CSF, i.e. blank gels and gels containing control AuNPs, did not mediate substantial cell accumulation (Figure 3A). Gels delivering free GM-CSF contained ~1.6×10^6 cells at day 3, and the number of cells in the gels remained higher than in the conditions without GM-CSF for the rest of the timecourse. Strikingly, when GM-CSF was conjugated to AuNPs and delivered in gels, over 5×10^6 cells accumulated in the gels at the peak of cell infiltration (Figure 3A). While the number of cells in the gels decreased after day 3, there were still close to 3×10^6 cells in the gels at day 5, and ~10^6 cells were maintained in the gels up until 14 days after injection. AUCs were calculated to estimate the total number of cells residing in the gels over the course of two weeks (Figure 3B). Gels delivering GM-CSF conjugated to AuNPs had an AUC of ~24×10^6, which was significantly higher than all of the other conditions. The AUC for gels delivering soluble GM-CSF was ~12×10^6, which was 2-fold lower than for the gels delivering GM-CSF conjugated to AuNPs. Although the gels with soluble GM-CSF exhibited more cell infiltration than blank gels or gels with control AuNPs, the differences in AUCs were not statistically significant.

To determine whether the structural properties of the pore-forming gels had a significant impact on cell infiltration into the material, the volume fraction of the porogens, as well as the total gel volume, were altered. A porogen volume fraction of 50% led to significantly more cell accumulation than a 25% porogen volume, which indicated that the incorporation of degradable porogens facilitated cell infiltration into the gels (Figure 3C). Unexpectedly, 3 days after injection of the gels, at the peak of cell infiltration, a 50% porogen fraction allowed significantly more cell infiltration than a higher 75% porogen fraction. When the porogen volume fraction was maintained at 50%, doubling the total volume of the gels from 100 μL to 200 μL led to significantly higher cell infiltration at later timepoints, i.e. days 5 and 10, even though the amount of GM-CSF delivered remained constant. The 100 μL gels with a 50% porogen volume fraction, which exhibited an accumulation of millions of cells over several days, were used for subsequent experiments.

Significant Enrichment of $CD11c^+$ DCs Among Infiltrating Cells

The cells isolated from this gel system were characterized by analyzing a variety of surface markers associated with immune cells. For all the timepoints and conditions examined, the vast majority of cells (~80–98%) were $CD11b^+$ (Figure 4C). A very high percentage of the cells across all timepoints and conditions were also $CD11c^+$ (Figure 4D). At day 3, the gels delivering GM-CSF conjugated to AuNPs contained 68% $CD11c^+$ cells, which was

significantly lower than the 89% $CD11c^+$ cells found in the gels delivering soluble GM-CSF. However, by day 5, the fraction of $CD11c^+$ cells in gels with GM-CSF + AuNP increased to 94% (Figure 4D), and virtually all of these cells were $CD11b^+$ $CD11c^+$ double positive (Figure 4A). In terms of absolute cell numbers, over 4 million $CD11c^+$ cells were present in the gels at day 3, the peak of cell infiltration (Figure 4H, Supporting Figure S6). Although the total number of infiltrating cells decreased after day 3 (Figure 3A), the number of $CD11c^+$ cells remained significant, with 2.3×10^6 $CD11c^+$ cells found at day 5, 0.9×10^6 at day 10, and 0.7×10^6 at day 14 (Figure 4H, Supporting Figure S6). Histological examination demonstrated that cells were able to infiltrate all the way into the center of the gels as early as 3 days after gel injection (Figure 4B), and also confirmed that these cells expressed CD11c. A substantial percentage of the $CD11b^+$ $CD11c^+$ double positive cells in the gels also expressed F4/80, a marker of macrophages that is also expressed on some DC subsets (Figure 4E). The gels delivering GM-CSF conjugated to AuNPs showed a trend towards a lower fraction of $F4/80^+$ cells compared to the other conditions, with some of these differences being statistically significant at days 3 and 10. At day 3, the peak of cell infiltration, around 30% of the cells expressed Gr-1, a marker of monocytes and granulocytes, when GM-CSF conjugated to AuNPs was delivered in the gels (Figure 4F). This was significantly higher than in the other conditions, which only had ~8–20% $Gr\text{-}1^+$ cells at this same timepoint. At later timepoints, this population was reduced and constituted less than 5% of the cells found in gels delivering GM-CSF + AuNP. Finally, the fraction of cells positive for DX5, an antibody clone that binds to CD49b and labels NK cells, as well as some NKT cells and T cells, was examined. At day 5, the fraction of cells positive for DX5 was only 5% in gels delivering GM-CSF + AuNP, which was significantly lower than in the conditions that did not contain GM-CSF (Figure 4G). However, at day 14, this relationship was reversed, such that gels delivering GM-CSF + AuNP contained significantly more $DX5^+$ cells, around 25%, than the other conditions. Overall, the data showed that pore-forming gels delivering GM-CSF were predominantly infiltrated by $CD11b^+$ $CD11c^+$ DCs (Figure 4A), of which a large fraction were also $F4/80^+$.

Immature Phenotype Exhibited by Infiltrating DCs

To evaluate the maturation level of these DCs, a number of cell surface markers associated with DC maturation were examined (Figure 5). Over 50% of the $CD11b^+$ $CD11c^+$ DCs isolated from the gels expressed MHCII, confirming their status as professional APCs (Figure 5A). In gels delivering GM-CSF, 30–40% of the $CD11c^+$ cells also expressed CD86 (Figure 5C). At day 3, both the percentage of $CD86^+$ cells, as well as the level of CD86 expression on these cells, were significantly lower in gels delivering GM-CSF (either GM-CSF alone or GM-CSF + AuNP) compared to control gels (blank or control AuNP) (Figure 5C, D). This trend was also visible at day 5, although not all of the differences were statistically significant. Over time, the percentage and expression levels of the $CD86^+$ cells in the control gels decreased and normalized to the levels seen in the GM-CSF loaded gels. For MHCII, a similar trend was seen for the expression levels, where the DCs infiltrating gels delivering GM-CSF expressed significantly less surface MHCII compared to the controls at day 3 (Figure 5B). As with CD86, the expression of MHCII eventually normalized to the same low level for all conditions at later timepoints. In terms of the percentage of $MHCII^+$ cells, however, a different trend was observed (Figure 5A). At day 3,

gels delivering GM-CSF alone had the highest percentage of $MHCII^+$ DCs. At day 5, the fraction of $MHCII^+$ DCs increased for all conditions. At days 10 and 14, the fraction of $MHCII^+$ cells was maintained for the control conditions, but decreased significantly in the gels delivering GM-CSF. At day 3, ~12% of the $CD11c^+$ cells also expressed CCR7 (Supporting Figure S7A). At subsequent timepoints, the fraction of $CCR7^+$ cells increased to approximately 20–30%, but the level of expression remained low (Supporting Figure S7A, B). There were no significant differences in the percentage or expression levels of CCR7 between conditions.

To further characterize the phenotype of the DCs infiltrating these gels, additional cell surface markers were examined at day 3. $CD11c^+$ DCs isolated from the gels expressed high levels of the negative costimulatory molecules PD-L1 and PD-L2 (Figure 5E). Gels delivering GM-CSF + AuNP contained over 90% $PD\text{-}L1^+$ and ~55% $PD\text{-}L2^+$ DCs, which was significantly higher than in the AuNP only control gels. A substantial fraction of $CD11c^+$ DCs also expressed PDCA-1, but GM-CSF delivery led to reduced PDCA-1 expression (~40%) compared to control gels (~80%) (Supporting Figure S7C). In gels delivering GM-CSF, only a small fraction of cells expressed the other markers that were analyzed, namely CD205 (DEC-205) (~12%), CD207 (langerin) (5%), CD103 (4%), and $CD8a^+$ (<1%) (Supporting Figure S7C).

Discussion

The results of this study demonstrate that a biomaterial delivery system can be engineered to locally enrich DCs *in vivo* without inducing their maturation or activation. The material system described here was based on non-inflammatory, injectable, pore-forming alginate hydrogels. These gels were characterized, and their fabrication parameters were altered to obtain porogens that degraded substantially within 3–5 days, leading to *in situ* pore formation within the bulk gel.

In addition to serving as a physical scaffold for cell infiltration, the pore-forming hydrogels were also used to deliver the cytokine GM-CSF. The rate of GM-CSF release from the hydrogels was modulated to obtain either a burst release or a more sustained, gradual release. Unlike certain heparin-binding proteins, such as VEGF,[27,28] GM-CSF does not interact with alginate and was rapidly released from alginate hydrogels. Sustained release of GM-CSF was achieved by conjugating GM-CSF to AuNPs prior to incorporation in the bulk, non-degrading phase of the gels. AuNPs form covalent bonds to thiol groups on the surface of proteins, and immobilized proteins are only released following spontaneous dissociation of the gold-thiol bonds.[29] In addition, 13 nm AuNPs are retained within alginate hydrogels, which exhibit a mesh size on the order of 5–6 nm.[30] Some loss of GM-CSF occurred in the process of conjugating GM-CSF to AuNPs, likely due to non-specific adsorption of protein and AuNPs onto plastic surfaces, despite the use of low protein binding disposables. However, a substantial amount of GM-CSF remained associated with the particles. GM-CSF conjugated to AuNPs and incorporated into alginate gels was released in a sustained manner and remained highly bioactive, demonstrating that the formation and dissociation of gold-thiol bonds did not lead to protein unfolding or denaturation.

Controlling the release of GM-CSF from the material led to greatly enhanced cell infiltration into the gels *in vivo*. Over 5×10^6 cells accumulated in pore-forming alginate gels delivering GM-CSF conjugated to AuNPs at the peak of cell infiltration, which was significantly higher than in gels delivering free GM-CSF. Although GM-CSF conjugated to AuNPs had a much more potent effect on cell accumulation *in vivo* than free GM-CSF, this effect cannot be attributed to the AuNPs themselves, since gels containing AuNPs conjugated to a control protein did not induce substantial cell accumulation above the blank gels. This is consistent with reports showing that gold nanoparticles are non-cytotoxic and non-immunogenic to macrophages[31] and DCs[32] *in vitro*. Gold is known to be biologically inert, with a long track record of safety as a dental filling material, and it has also been used clinically in the treatment of rheumatoid arthritis, an autoimmune disease.[33] The strategy of using AuNPs as carriers could potentially be employed to modulate the release of other non-heparin-binding proteins from alginate hydrogels.

Tuning the physical properties of the hydrogels also had a significant impact on *in vivo* cell infiltration. In this study, an intermediate porogen volume fraction of 50% was optimal for achieving maximal cell accumulation within the gels. At a lower porogen volume fraction, the gels contained significantly fewer cells, supporting the importance of creating a macroporous structure to allow effective cell infiltration. However, increasing the porogen volume fraction beyond 50% did not further improve cell accumulation, possibly because the bulk gel may collapse as the porogens degrade when the porogen fraction is too high, resulting in sub-optimal cell infiltration. Although the incorporation of 50% degradable porogens by volume led to a significant increase in the interconnected porosity of the gels, the level of interconnected porosity achieved was not as high as what has been seen in other macroporous gel systems.[17] However, cells are still able to infiltrate into the center of the gels after only 3 days *in vivo*, indicating that even a modest level of interconnected porosity enables effective cell infiltration in this system. In addition, the actual interconnected porosity *in vivo* may be higher, since the gels are subject to mechanical stresses exerted by tissues and infiltrating cells, which may lead to the formation of local fractures within the gels and the creation of new connections between pores.

Strikingly, a very high percentage of the cells infiltrating this material system consisted of $CD11b^+$ $CD11c^+$ DCs. At day 5, more than 90% of the cells in the gels were double positive for CD11b, a broadly expressed marker for leukocytes, and CD11c, a characteristic marker of conventional DCs. This percentage is far higher than what has been achieved using comparable doses of GM-CSF in other material systems.[7,34] PLGA[7] and mesoporous silica[34] based scaffolds were shown to recruit substantial numbers of DCs in response to delivery of GM-CSF (1–3ug) and elicit cellular immune responses against antigens of interest. However, the percentage of $CD11c^+$ DCs infiltrating those materials did not exceed 30% at any of the timepoints analyzed, which is consistent with the notion that materials such as PLGA and silica elicit an innate immune response, resulting in significant infiltration by other cell types besides DCs. In the system described here, the pronounced enrichment of DCs can likely be attributed to the use of non-inflammatory materials, as well as the intentional absence of adhesion ligands on the alginate polymer forming the gels, which may favor infiltration by immune cells. Most other mammalian cell types require adhesion ligands for survival and migration. Leukocytes, on the other hand, can traffic in an

integrin-independent manner by amoeboid migration.[35–37] As a result, the gels may be selectively restricting infiltration by fibroblasts and other cells from neighboring tissues, such that the gels are infiltrated almost exclusively by DCs. The ability to manipulate a highly uniform and enriched population of DCs is an attractive feature for biomaterial-based vaccines, since it could allow more precise and potent downstream responses, either directed towards immunity or tolerance. It could also be of great interest and utility to extend this approach to recruit other immune cell types, such as T and B cells, using different chemokines or lymphokines.

The DCs infiltrating the hydrogels *in vivo* were characterized, and their cell surface marker profile was consistent with that of immature DCs. The $CD11c^+$ DCs isolated from the gels expressed MHCII, CD86, and CCR7, but at low levels, comparable to those seen on immature BMDCs. Although these markers can be indicative of DC maturation or activation when expressed at high levels, some level of MHCII and CCR7 expression may be important for inducing antigen-specific tolerogenic responses.[3] CCR7 mediates homing to the lymph nodes, where the DCs interact with T cells, and MHCII is necessary for peptide presentation by DCs to $CD4^+$ helper and regulatory T cells. Interestingly, CD86 expression levels were significantly lower in gels delivering GM-CSF, either with or without AuNPs, compared to gels without GM-CSF, suggesting that GM-CSF may be suppressing maturation. This is consistent with previous reports showing that high GM-CSF concentrations in the absence of danger signals can suppress activation of dendritic cells both *in vitro* and *in vivo*.[7] The DCs infiltrating the gels also expressed high levels of PD-L1 and PD-L2, two negative costimulatory molecules that signal through PD-1 on T cells and are important for tolerance mechanisms.[38,39] This is a promising indication that the DCs infiltrating the gels may have the capacity to induce tolerance.

Overall, the cell surface marker profile of the DCs in the gels indicates that the material system used here did not generate an inflammatory environment. Although reports in the literature concerning the immunogenicity of alginate are conflicting, studies performed using highly purified, medical grade alginate show that the polymer does not induce immune cell activation.[15,40] A recent study, while confirming that the alginate polymer itself does not cause DC activation, has also shown that Ca^{2+}, which is commonly used to ionically crosslink alginate hydrogels in a biocompatible manner, can potentiate inflammatory responses.[41] However, the immunostimulatory effect of Ca^{2+} released from gels alone was small compared to the enhancing effect it had on DC activation when it was delivered together with bacterial lipopolysaccharide (LPS), a potent danger signal. In addition, the location of the subcutaneous gel injection *in vivo* had a marked influence on the effects of Ca^{2+}, with lateral injection (along the side of the body) leading to significantly less secretion of inflammatory cytokines compared to medial injection (along the midline on the back).[41] In the system described here, Ca^{2+} is expected to minimally impact DC activation, since the gels were injected laterally *in vivo* and did not deliver any danger signals.

Although the precise subtype and lineage of the DCs in this system remains unclear, analysis suggests that they may represent a population of $CD11b^+$ migratory or monocyte-derived DCs. Despite the fact that the gels were injected subcutaneously and were adjacent to the dermis, the majority of cells infiltrating the gels did not express CD207 (i.e. langerin) or

CD103, two markers that are used to characterize specific populations of Langerhans cells and dermal DCs. At early timepoints, however, a fraction of $CD11b^+$ cells expressed Gr-1, a marker of monocytes and granulocytes. Few cells co-expressed CD11c and Gr-1, and the $Gr\text{-}1^+$ cells had a forward scatter (FSC) / side scatter (SSC) profile when analyzed by flow cytometry that appeared consistent with monocytes. In all conditions, as $Gr\text{-}1^+$ decreased over time, the percentage of $CD11c^+$ cells increased, suggesting a transition between the resident cell populations. It could be speculated that these $Gr\text{-}1^+$ cells represented a population of monocytes or pre-DCs that migrated and differentiated into $CD11c^+$ DCs upon exposure to GM-CSF.

Conclusions

This study demonstrates that an injectable, non-inflammatory polymeric delivery system can be engineered to locally enrich millions of immature DCs *in vivo*. Alginate hydrogels that form pores *in situ* were designed to deliver the cytokine GM-CSF in a sustained manner. Following injection of these pore-forming gels *in vivo*, substantial cell infiltration was obtained by controlling both the release kinetics of GM-CSF, as well as the physical structure of the hydrogel. Several million cells accumulated in the gels, and the majority of these cells consisted of $CD11b^+$ $CD11c^+$ DCs. Further analysis of cell surface marker expression revealed that these DCs were immature and expressed negative costimulatory molecules, suggesting that these DCs may be competent to induce immune tolerance if presented with an appropriate antigen. This work may provide the basis for further development of a highly effective and therapeutic antigen-specific tolerogenic vaccine.

Experimental Section

Animals

All work involving C57BL/6J mice (female, aged 6–10 weeks; Jackson Laboratories) was performed in compliance with National Institutes of Health and institutional guidelines.

Alginate Modification

Medical grade, high guluronic acid content, high molecular weight alginate (MVG) (FMC Biopolymers) was subjected to 7.5% oxidation and reduction, as described previously.[18,42] Briefly, alginate (1 g) was dissolved in water (100 mL) to obtain a 1% solution. Sodium periodate (81 mg) was added while stirring at room temperature, and the reaction was shielded from light. After 17 h, the reaction was quenched by the addition of ethylene glycol (23.25 μL). The aldehyde groups on the oxidized alginate were then reduced by adding sodium borohydride (14.2 mg) while stirring at room temperature. After 2 h, the pH was adjusted to 7.4 by adding diluted acetic acid. Alginate was dialyzed against water using a 3,500 MWCO dialysis membrane (Spectrum Laboratories), then sterile-filtered, lyophilized, and stored at −20°C until use.

Alginate Porogen Fabrication

Porogens were fabricated using a 2% w/v solution of 7.5% oxidized and reduced alginate together with varying amounts of unmodified MVG alginate (0%, 0.05%, 0.25%, or 0.75%,

as specified). Alginate was reconstituted in DMEM while stirring at 4°C overnight. Porogens were formed by dispensing the alginate solution through a glass nebulizer while applying a coaxial flow of N_2 gas (5.2 SLPM, unless specified otherwise), and collecting the beads in a crosslinking solution of 100 mM $CaCl_2$ and 100 mM HEPES (pH 7.2). After crosslinking for 5 min, beads were washed 3 times by resuspending in an excess of HBSS (Hank's Balanced Salt Solution, Sigma Aldrich) and pelleting at 1,800 *g*.

AuNP Synthesis and Characterization

AuNPs were synthesized via a citrate-reduction method.[43] Briefly, a 250 mL erlen-meyer flask containing a 2" stir bar was cleaned by rinsing briefly in aqua regia (1 part nitric acid: 3 parts hydrochloric acid) and subsequently rinsing thoroughly in MilliQ-filtered (Millipore) H_2O. A solution of 0.01% w/v gold chloride (III) chloride hydrate (Sigma Aldrich #254169) in H_2O (100 mL) was added to the flask and brought to a boil on a heating and stirring plate set to 400°C and 500 rpm. A 1% w/v sodium citrate tribasic dihydrate (Sigma Aldrich # 4641) solution (3 mL) was rapidly added by dispensing forcefully through a needle (18G) attached to a syringe (10 mL). The solution was removed from the stirring/heating plate once its color changed to red. The size of the synthesized AuNPs was determined by dynamic light scattering (DLS) on a Malvern Zen 3600 Zetasizer, and their concentration was determined by measuring absorbance at 518–519 nm on a UV spectrophotometer.

AuNP Conjugation

A sterile-filtered AuNP solution (525 μL, 45 μg mL^{-1}) was concentrated 157.5-fold by centrifuging at 20,000*g* for 20 min and removing supernatant. After resuspending the particles by pipetting and sonicating in a water bath sonicator for 10 min, concentrated AuNPs (3.33 μL) were mixed with recombinant murine GM-CSF (3 μg, 1 mg mL^{-1} in dH_2O; Peprotech# 315-03) and incubated at 37°C for 1 h to allow formation of the gold-sulfur bonds. The amount of GM-CSF to be conjugated to AuNPs was determined by calculating the theoretical geometric packing of GM-CSF molecules on the surface of the AuNPs. The diameter of AuNPs was 13 nm, as measured by DLS (see above). The diameter of GM-CSF was estimated to be 3.4 nm based on its molecular weight, assuming it is a globular protein. 150% of the theoretical amount required to obtain full coverage was used to promote complete coverage of AuNPs.

Alginate Hydrogel Fabrication

A solution of 3% w/v unmodified alginate in DMEM without L-cystine (Sigma Aldrich) was reconstituted while stirring at room temperature overnight. The 3% w/v alginate solution was mixed with additional cystine-free DMEM containing either no protein (for blank gels), free GM-CSF, or GM-CSF-loaded AuNPs, resulting in a final concentration of 2% w/v unmodified alginate. This mixture, which constituted the bulk phase of the gels, was then mixed with pre-formed porogen beads. Finally, the bulk gel was crosslinked by mixing with a sterile calcium sulfate slurry (1.2 M $CaSO_4 \cdot 2H_2O$ in H_2O). The volume of $CaSO_4$ crosslinking solution used was 4% v/v relative to the bulk alginate. The volume fraction of porogens was 50% of the total gel volume, except when specified otherwise. All mixing steps were performed using luer-lock syringes (1 mL) joined with luer-lock connectors. For *in vitro* studies, the gels were immediately cast between two silanized glass plates separated

by 2 mm spacers. After allowing the gels to crosslink for 20 min, gel disks were punched out using a sterile 8 mm biopsy punch to form ~100 μL gels. For *in vivo* studies, a needle (18G) was attached to the syringe and gels were injected subcutaneously immediately after crosslinking the bulk phase of the gel (within approximately 30–60 sec). The gels stayed in place after injection.

Confocal Microscopy

Images were taken using an upright Zeiss LSM 710 confocal microscope, processed using ZEN software (Zeiss), and analyzed using ImageJ software (NIH).

Bulk Gel Degradation Assay

Alginate gels (100 μL) were incubated in release buffer at 37°C. At the indicated timepoints, gels were flash frozen and lyophilized to determine their dry mass.

Gel Wicking Assay

Nanoporous or pore-forming gels (100 μL) were incubated in media (1 mL) at 37°C. Water wicking was performed by touching an absorbent Kimwipe (Kimberly-Clark) to one side of the gel, allowing the water in the pores to be drawn out by capillary action. To measure the wicking volume, gels were gently placed on a disposable tray and weighed on a microbalance before and after wicking.

Pore-forming Gel Degradation Assay

Pore-forming alginate gels (100 μL) fabricated with FITC-labeled porogens were incubated in media (1 mL) at either 4°C or 37°C. At each timepoint, the media were collected and replaced with fresh media. The amount of FITC released at each timepoint was determined by measuring FITC fluorescence in the collected media samples using a BioTek plate reader.

In Vitro GM-CSF Release

Particles or gels loaded with GM-CSF (3 μg per sample) were incubated at 37°C in HBSS containing 1% BSA (Roche) to block non-specific protein adsorption and 1% penicillin/streptomycin. Whenever possible, low protein binding disposables were used, also to minimize non-specific protein adsorption. At each timepoint, the release buffer was collected and replaced with fresh buffer (1 mL). The amount of GM-CSF released at each timepoint, as well as the amount of unreleased GM-CSF still associated with the material after 4 weeks, were determined by ELISA (R&D).

In Vitro GM-CSF Bioactivity Assay

Bone marrow was isolated from C57BL/6J mice, dissociated into a single-cell suspension, and resuspended in RPMI-1640 media (supplemented with 10% heat-inactivated FBS, 1% penicillin/streptomycin, 50 μM β-mercaptoethanol). Bone marrow cells (4×10^4 cells per well in 100 μL) were seeded in black tissue culture treated 96-well plates. GM-CSF standards or unknown samples (100 μL) were added, in triplicate, to each well, bringing the final volume to 200 μL per well. The standard curve, which was prepared by performing 4-fold serial dilutions of a stock solution of GM-CSF, spanned concentrations ranging from 4

ng per well to 0.98 pg per well. Cells were cultured at 37°C for 5 days, at which point 10% v/v of AlamarBlue reagent (Life Technologies) was added to each well. After a 4 h incubation at 37°C, plates were read on a BioTek plate reader to measure the absorbance at 490 nm. The standard curve was used to determine the level of bioactivity of the experimental samples in " μg equivalent". "Percent bioactivity" was calculated by normalizing the " μg equivalent" activity measured in the bioactivity assay to the amount of GM-CSF, in μg, detected by ELISA for the same samples.

In Vivo Studies

In vivo studies were done in C57BL/6J female mice between 6–10 weeks of age. Gels were injected subcutaneously into one flank. At various timepoints, gels were removed and dissociated in EDTA (40 mM in PBS) on ice for 10 min, with periodic vortexing. Cells were filtered through 40 μm cell strainers, and live cells were counted using a Countess automated cell counter (Life Technologies).

Flow Cytometry

Cells were blocked with Fc Block (BioLegend) for 15 min and stained with antibodies (BioLegend, eBioscience, or BD Biosciences) for 30 min. The antibodies used were specific for CD11b (clone M1/70), CD11c (clone N418), F4/80 (clone BM8), Gr-1 (clone RB6-8C5), DX5 (clone DX5), MHC II (I-A/I-E) (clone M5/114.15.2), CD86 (clone PO3), CCR7 (clone 4B12), PD-L1 (clone 10F.9G2), PD-L2 (clone TY25), PDCA-1 (clone eBio927), CD207 (clone 4C7), CD205 (NLDC-145), and CD103 (clone 2E7). 7-AAD (BioLegend) or Fixable Live/Dead dyes (Life Technologies) were used for live and dead cell discrimination. All blocking and antibody staining steps were performed in flow cytometry staining buffer consisting of PBS with 0.5% BSA and 2 mM EDTA at 4°C (except for CCR7 staining, which was performed at 37°C, as recommended by the manufacturer). Data were collected on either LSRII or LSRFortessa flow cytometers (BD Biosciences) and analyzed using FlowJo software (TreeStar).

Immunofluorescent Staining of Frozen Sections

Gels were fixed in fresh, ice-cold 4% PFA in PBS at 4°C for 1 h, then rinsed in PBS at 4°C for 2–3 h. Sucrose infiltration was performed by incubating the gels in 30% w/v sucrose in PBS at 4°C overnight. Before embedding, gels were incubated in a 1:1 mixture of 30% w/v sucrose and OCT (Tissue-Tek) for 1 h. Gels were embedded in OCT in disposable molds and stored at -80°C until sectioning on a Leica cryostat. 10 μm sections were cut and collected on Superfrost Plus glass slides (VWR). For staining, sections were first hydrated in PBS for 5 min and permeabilized in 0.5% Triton X-100 in PBS for 5 min. All subsequent washes were performed using a staining buffer consisting of 0.1% Triton X-100 in PBS. Slides were blocked for 30 min at room temperature in blocking buffer (staining buffer + 10% serum from the same species as the secondary antibodies). Primary antibodies were applied to slides in 150 μL of blocking buffer and incubated at 4°C overnight, after which the slides were washed for 3–4 h at 4°C. Secondary antibodies were applied to slides in 300 μLof blocking buffer and incubated at room temperature for 1 h, then washed for 1 h. Nuclei were counterstained using a 1:1000 dilution of Hoechst 33342 (Life Technologies).

Statistical Analysis

When comparing two groups, a two-tailed Student's t-test was used. When comparing multiple groups, a one-way or two-way analysis of variance (ANOVA) was performed with corrections for multiple comparisons. All statistical analyses were performed using Prism 6 (GraphPad).

Supplementary Material

Refer to Web version on PubMed Central for supplementary material.

Acknowledgements

This work was supported by the JDRF (5-2011-434) and the National Institutes of Health (NIH) (1R01DE019917). The authors would like to thank Dr. Nathaniel Huebsch and Christopher Madl for their help with the pore-forming gels, and Dr. Ovijit Chaudhuri for providing FITC-labeled alginate. We would like to acknowledge Dr. Jaeyun Kim, Dr. Cathal Kearney, and Weiwei Aileen Li for their help with gold nanoparticle synthesis and characterization. We also thank Dr. Omar Ali and Dr. Roger Warren Sands for scientific discussions.

References

1. Steinman RM, Turley S, Mellman I, Inaba K. J. Exp. Med. 2000; 191:411. [PubMed: 10662786]
2. Steinman RM, Hawiger D, Nussenzweig MC. Annu. Rev. Immunol. 2003; 21:685. [PubMed: 12615891]
3. Cools N, Ponsaerts P, Tendeloo VFIV, Berneman ZN. J Leukoc. Biol. 2007; 82:1365. [PubMed: 17711977]
4. Ohnmacht C, Pullner A, King SBS, Drexler I, Meier S, Brocker T, Voehringer D. J Exp. Med. 2009; 206:549. [PubMed: 19237601]
5. Getts DR, Martin AJ, McCarthy DP, Terry RL, Hunter ZN, Yap WT, Getts MT, Pleiss M, Luo X, King NJC, Shea LD, Miller SD. Nat. Biotechnol. 2012; 30:1217. [PubMed: 23159881]
6. Yeste A, Nadeau M, Burns EJ, Weiner HL, Quintana FJ. Proc. Natl. Acad. Sci. U. S. A. 2012; 109:11270. [PubMed: 22745170]
7. Ali OA, Huebsch N, Cao L, Dranoff G, Mooney DJ. Nat. Mater. 2009; 8:151. [PubMed: 19136947]
8. Miller SD, Turley DM, Podojil JR. Nat. Rev. Immunol. 2007; 7:665. [PubMed: 17690713]
9. Athanasiou KA, Niederauer GG, Agrawal CM. Biomaterials. 1996; 17:93. [PubMed: 8624401]
10. Anderson JM, Shive MS. Adv. Drug Deliv. Rev. 1997; 28:5. [PubMed: 10837562]
11. Drury JL, Mooney DJ. Biomaterials. 2003; 24:4337. [PubMed: 12922147]
12. Kretlow JD, Klouda L, Mikos AG. Adv. Drug Deliv. Rev. 2007; 59:263. [PubMed: 17507111]
13. Hoare TR, Kohane DS. Polymer. 2008; 49:1993.
14. Kim WS, Mooney DJ, Arany PR, Lee K, Huebsch N, Kim J. Tissue Eng. Part A. 2011; 18:737. [PubMed: 22011105]
15. Lee KY, Mooney DJ. Prog. Polym. Sci. 2012; 37:106. [PubMed: 22125349]
16. Hill E, Boontheekul T, Mooney DJ. Proc. Natl. Acad. Sci. 2006; 103:2494. [PubMed: 16477029]
17. Bencherif SA, Sands RW, Bhatta D, Arany P, Verbeke CS, Edwards DA, Mooney DJ. Proc. Natl. Acad. Sci. 2012; 109:19590. [PubMed: 23150549]
18. Huebsch N, Lippens E, Lee K, Mehta M, Koshy S, Darnell M, Desai R, Madl CM, Xu M, Zhao X, Chaudhuri O, Verbeke CS, Kim WS, Alim K, Mammoto A, Ingber DE, Duda GN, Mooney DJ. Nat. Mater. 2015 *In press*.
19. Inaba, K.; Swiggard, WJ.; Steinman, RM.; Romani, N.; Schuler, G.; Brinster, C. Curr. Protoc. Immunol. John Wiley & Sons, Inc.; 2001.
20. Ali OA, Tayalia P, Shvartsman D, Lewin S, Mooney DJ. Adv. Funct. Mater. 2013; 23:4621. [PubMed: 24688455]

21. Dranoff G. Immunol. Rev. 2002; 188:147. [PubMed: 12445288]
22. Parmiani G, Castelli C, Pilla L, Santinami M, Colombo MP, Rivoltini L. Ann. Oncol. 2007; 18:226. [PubMed: 17116643]
23. Cheatem D, Ganesh BB, Gangi E, Vasu C, Prabhakar BS. Clin. Immunol. Orlando Fla. 2009; 131:260.
24. Gaudreau S, Guindi C, Ménard M, Besin G, Dupuis G, Amrani A. J Immunol. Baltim. Md 1950. 2007; 179:3638.
25. Sheng JR, Li L, Ganesh BB, Vasu C, Prabhakar BS, Meriggioli MN. J Immunol. Baltim. Md 1950. 2006; 177:5296.
26. Zou T, Caton AJ, Koretzky GA, Kambayashi T. J Immunol. 2010; 185:2790. [PubMed: 20686126]
27. Silva EA, Mooney DJ. J Thromb. Haemost. 2007; 5:590. [PubMed: 17229044]
28. Lee KY, Peters MC, Anderson KW, Mooney DJ. Nature. 2000; 408:998. [PubMed: 11140690]
29. Bhatt N, Huang P-JJ, Dave N, Liu J. Langmuir. 2011; 27:6132. [PubMed: 21513322]
30. Boontheekul T, Kong H-J, Mooney DJ. Biomaterials. 2005; 26:2455. [PubMed: 15585248]
31. Shukla R, Bansal V, Chaudhary M, Basu A, Bhonde RR, Sastry M. Langmuir. 2005; 21:10644. [PubMed: 16262332]
32. Villiers CL, Freitas H, Couderc R, Villiers M-B, Marche PN. J Nanoparticle Res. 2009; 12:55.
33. Thakor A, Jokerst J, Zaveleta C, Massoud T, Gambhir S. Nano Lett. 2011; 11:4029. [PubMed: 21846107]
34. Kim J, Li WA, Choi Y, Lewin SA, Verbeke CS, Dranoff G, Mooney DJ. Nat. Biotechnol. 2015; 33:64. [PubMed: 25485616]
35. Wolf K, Müller R, Borgmann S, Bröcker E-B, Friedl P. Blood. 2003; 102:3262. [PubMed: 12855577]
36. Lämmermann T, Bader BL, Monkley SJ, Worbs T, Wedlich-Söldner R, Hirsch K, Keller M, Förster R, Critchley DR, Fässler R, Sixt M. Nature. 2008; 453:51. [PubMed: 18451854]
37. Friedl P, Weigelin B. Nat. Immunol. 2008; 9:960. [PubMed: 18711433]
38. Keir ME, Liang SC, Guleria I, Latchman YE, Qipo A, Albacker LA, Koulmanda M, Freeman GJ, Sayegh MH, Sharpe AH. J Exp. Med. 2006; 203:883. [PubMed: 16606670]
39. Keir ME, Butte MJ, Freeman GJ, Sharpe AH. Annu. Rev. Immunol. 2008; 26:677. [PubMed: 18173375]
40. Zimmermann U, Klöck G, Federlin K, Hannig K, Kowalski M, Bretzel RG, Horcher A, Entenmann H, Sieber U, Zekorn T. Electrophoresis. 1992; 13:269. [PubMed: 1396520]
41. Chan G, Mooney DJ. Acta Biomater. 2013; 9:9281. [PubMed: 23938198]
42. Silva EA, Kim E-S, Kong HJ, Mooney DJ. Proc. Natl. Acad. Sci. U. S. A. 2008; 105:14347. [PubMed: 18794520]
43. Perrault SD, Chan WCW. J Am. Chem. Soc. 2010; 132:11824.

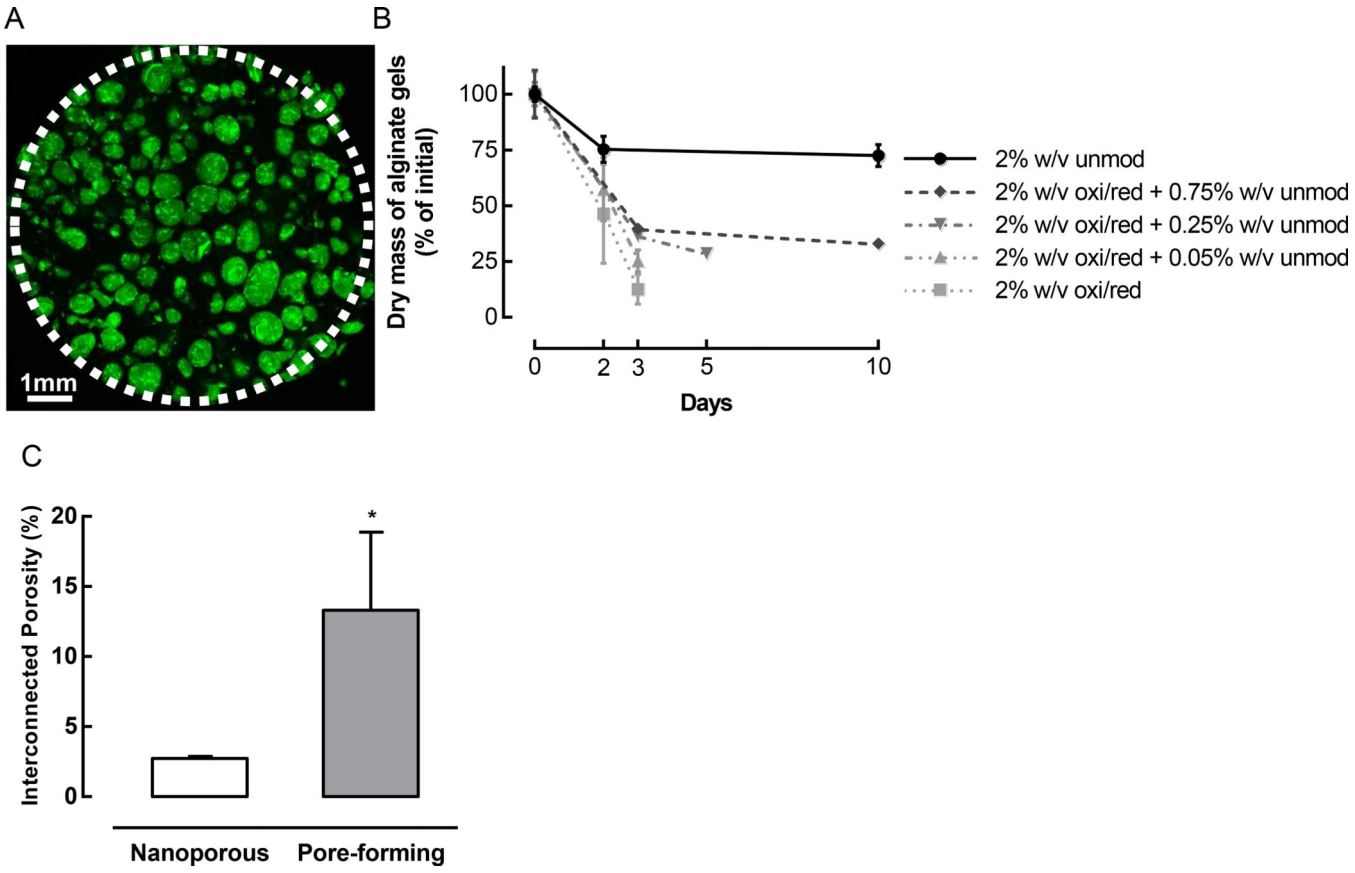

Figure 1.

Pore-forming hydrogels were created by incorporating rapidly degrading porogen beads into a bulk gel. (A) Confocal Z-slice of a pore-forming gel containing 50% v/v bulk gel (unmod alginate) and 50% v/v FITC-labeled porogen beads (green, fabricated using 2% w/v oxi/red + 0.25% unmod alginate). The white dotted line demarcates the border of the gel, which was sampled using a biopsy punch; some porogens at the edge of the gel were dislodged in the process of punching out the sample. (B) *In vitro* degradation kinetics of alginate gels consisting of 2% w/v unmodified (unmod) alginate, 2% w/v oxidized and reduced (oxi/red) alginate, or binary mixtures of oxi/red and unmod alginate. (n = 3; mean ± s.d. shown). (C) Interconnected porosity of nanoporous and pore-forming gels, as determined by a water wicking assay. Nanoporous gels consisted of 100% unmodified alginate, and pore-forming gels were composed of 50% v/v bulk gel (unmod alginate) and 50% v/v porogens (fabricated using 2% w/v oxi/red + 0.25% unmod alginate). (n = 4; mean ± s.d. shown; * $p < 0.05$).

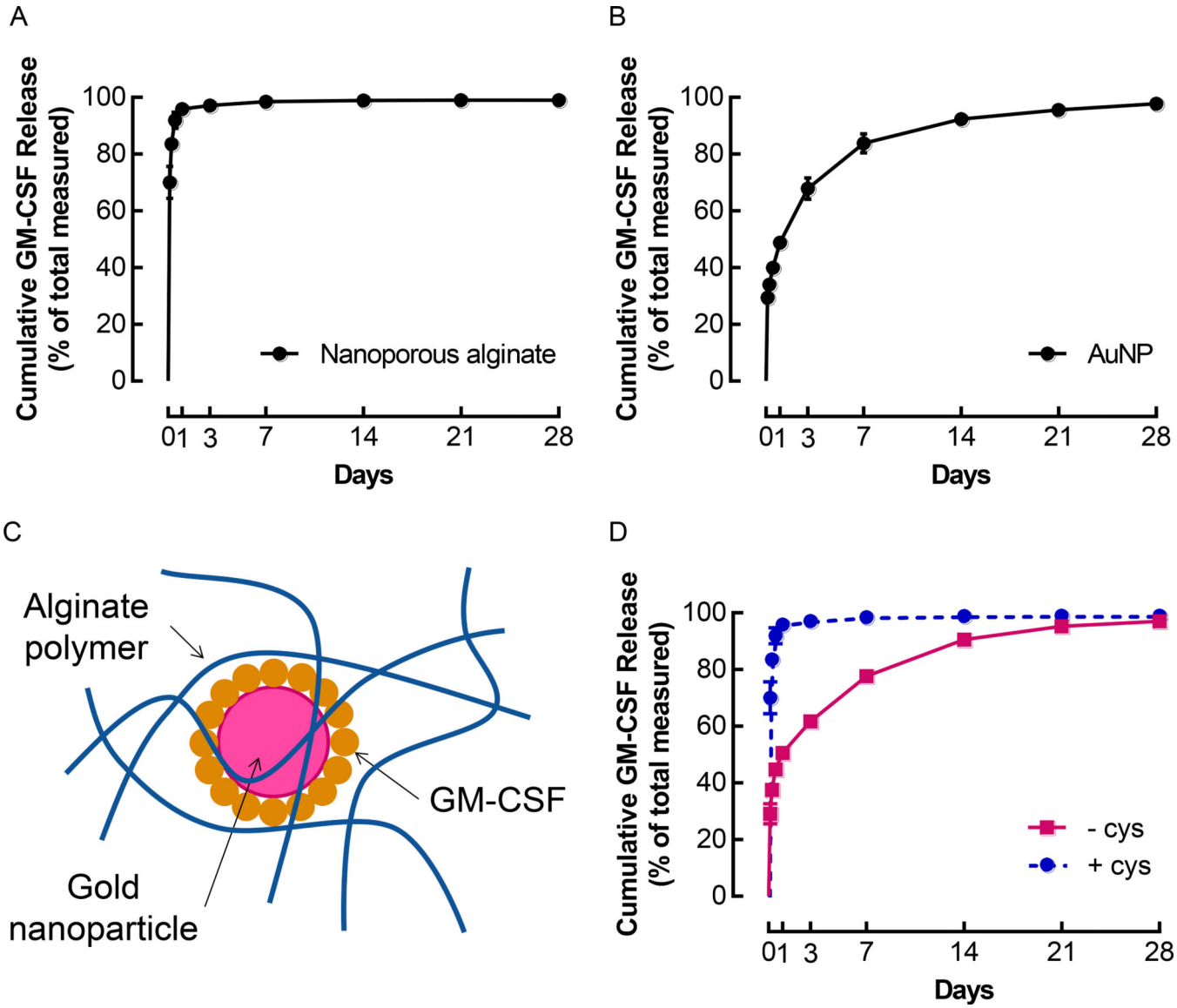

Figure 2.

Conjugation of GM-CSF to AuNPs allowed control over release kinetics. (A) Cumulative GM-CSF release after direct incorporation of 3 μg GM-CSF in nanoporous, ionically crosslinked alginate gels. (n = 5; mean ± s.d. shown). (B) Cumulative GM-CSF release after conjugation of 3 μg GM-CSF to AuNPs. (n = 5; mean ± s.d. shown). (C) Diagram of GM-CSF conjugated AuNPs incorporated in an alginate polymer network. (D) Release of GM-CSF from 100 μL nanoporous alginate gels containing AuNPs that were conjugated with 3 μg of GM-CSF and formulated either with or without cystine. (n = 5; mean ± s.d. shown).

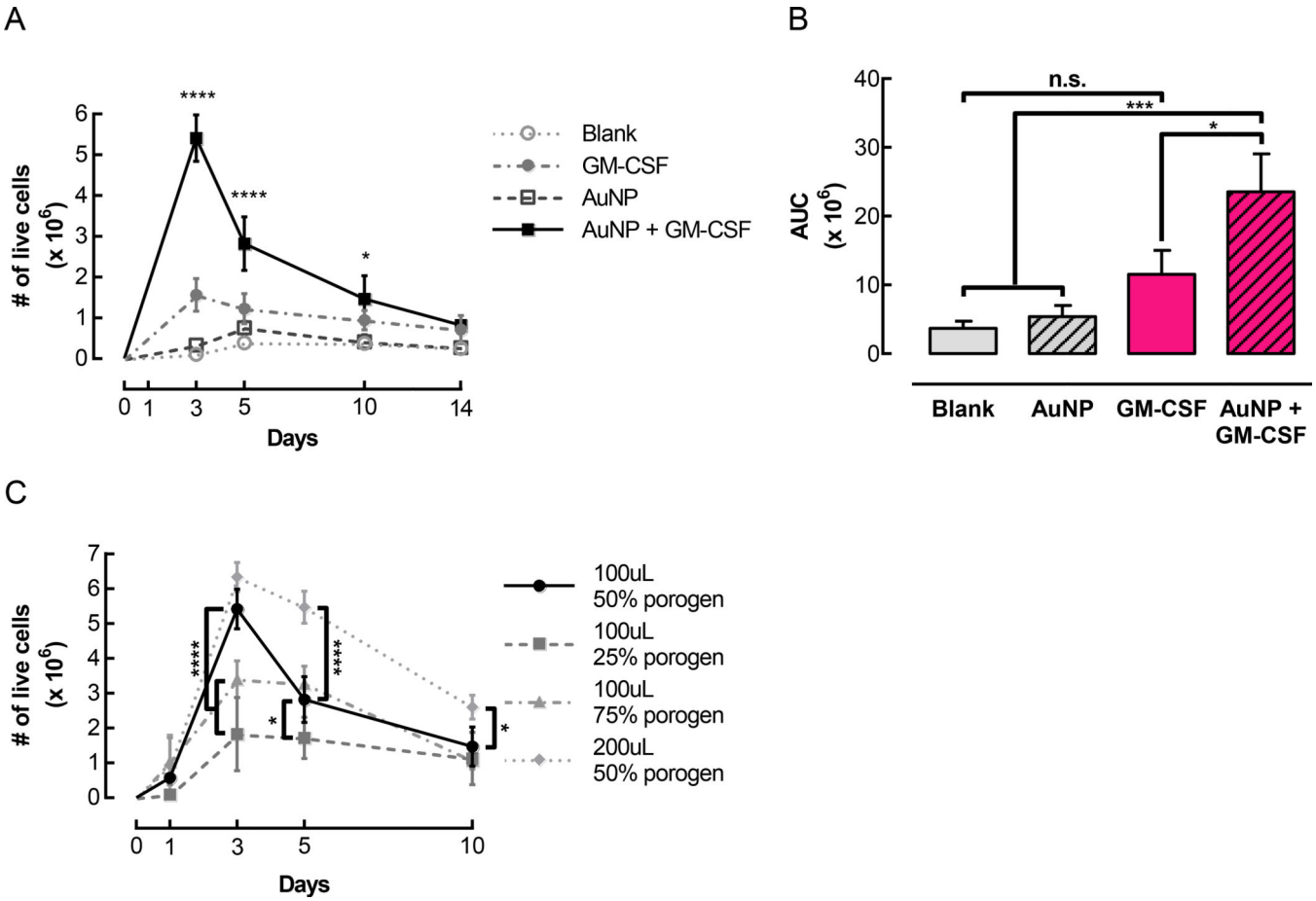

Figure 3.

Pore-forming gels delivering GM-CSF conjugated to AuNPs mediated substantial cell accumulation *in vivo*. Gels were injected subcutaneously into the flanks of C57BL/6J mice. At specified timepoints, gels were dissociated to retrieve and quantify infiltrating cells. (A) Number of live cells isolated over time from control gels (Blank and AuNP) and gels loaded with 3 μg GM-CSF either directly incorporated in the gels (GM-CSF) or first conjugated to AuNPs (AuNP + GM-CSF). For all conditions, pore-forming gels contained a 50% porogen volume fraction. (n = 3 – 9 per condition per timepoint; mean ± s.d. shown; * $p < 0.05$ compared to Blank and AuNP; **** $p < 0.0001$ compared to all other conditions; AuNP + GM-CSF condition was compared to all other conditions at each timepoint.) (B) Areas under curves corresponding to the data shown in (A). (* $p < 0.05$; *** $p < 0.001$; all conditions were compared to each other.) (C) The total volume and porogen volume fraction of pore-forming gels were varied, and infiltrating cells were quantified at specified timepoints. (n = 3 – 9 per condition per timepoint; mean ± s.d. shown; * $p < 0.05$; **** $p < 0.0001$; 100 μL 50% porogen condition was compared to all other conditions at each timepoint.)

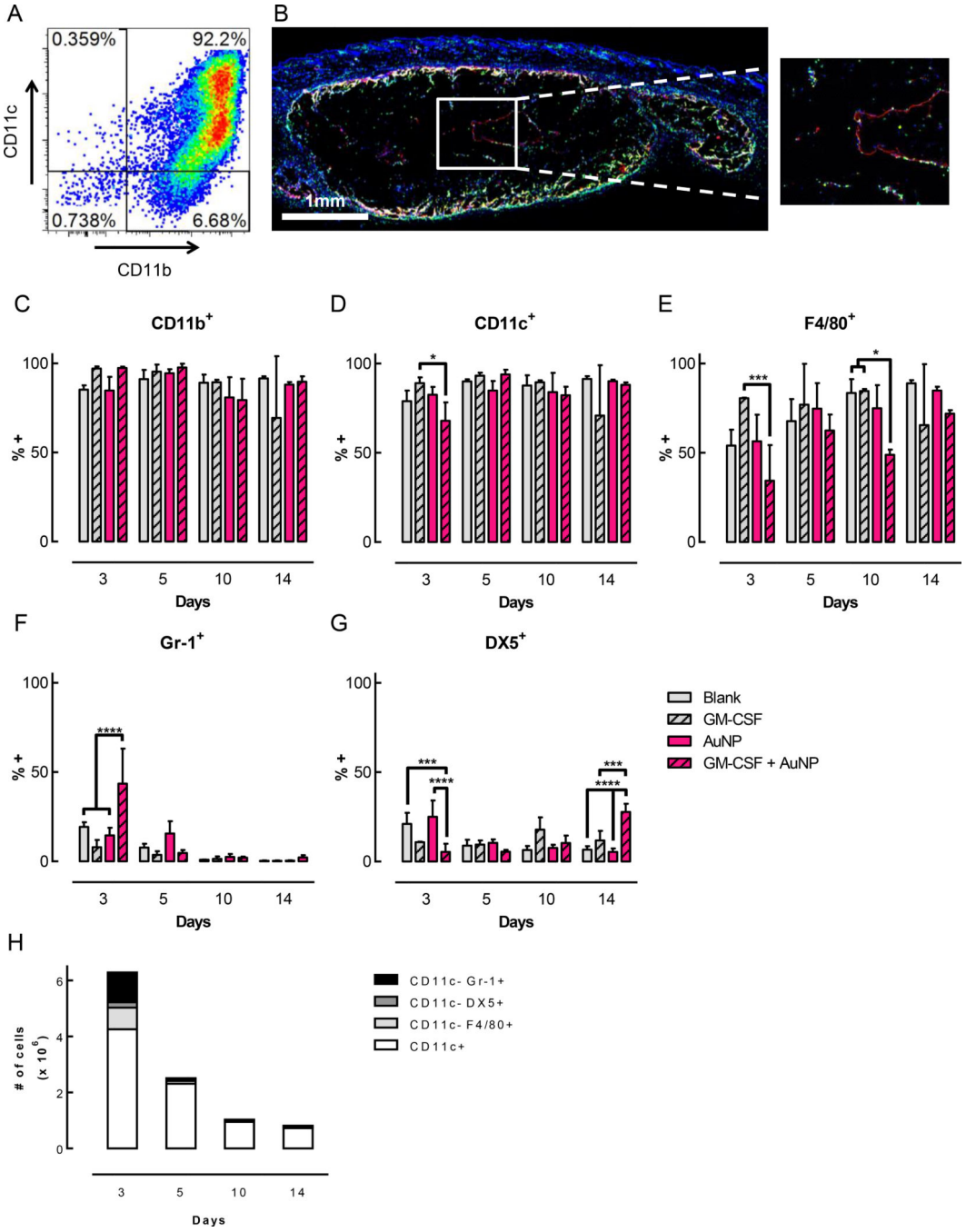

Figure 4.

Gels delivering GM-CSF *in vivo* contained a highly enriched population of DCs. Pore-forming gels (50% porogen volume fraction, loaded with 3ug GM-CSF) were injected subcutaneously into the flanks of C57BL/6J mice. At specified timepoints, gels were dissociated to retrieve and characterize infiltrating cells. (A) Flow cytometry plot of $CD11b^+$ $CD11c^+$ cells isolated from a gel delivering GM-CSF + AuNPs after 5 days. (B) Immunofluorescent staining of a sectioned gel delivering GM-CSF + AuNPs 3 days after injection. 10 μm sections were stained for CD11c (red), MHCII (green), and nuclei (blue).

(C-G) Frequency of cells expressing cell surface markers CD11b (C), CD11c (D), F4/80 (E), Gr-1 (F), and DX5 (G). Representative FACS plots for day 5 shown in Supporting Figure S8. (n = 3 per condition per timepoint; mean ± s.d. shown; * $p < 0.05$; *** $p < 0.001$; **** $p < 0.0001$; GM-CSF + AuNP condition was compared to all other conditions at each timepoint.) (H) Absolute numbers of cells isolated from gels delivering GM-CSF + AuNPs expressing different cell surface markers. (n = 3–6 per condition per timepoint; mean shown.)

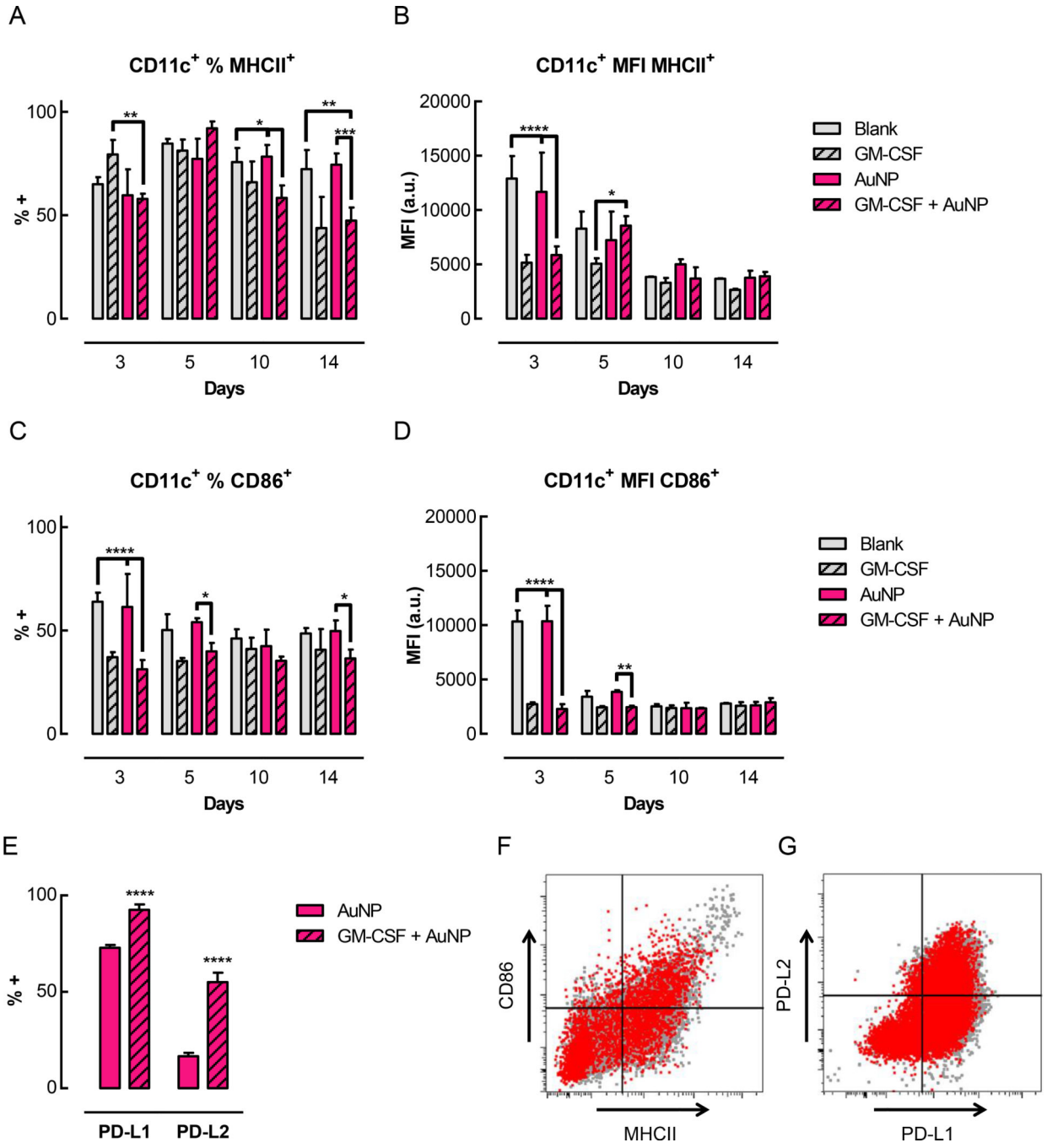

Figure 5.

DCs residing in the gels exhibited an immature phenotype. Pore-forming gels (50% porogen volume fraction, loaded with 3ug GM-CSF) were injected subcutaneously into the flanks of C57BL/6J mice; at specified timepoints, gels were isolated and dissociated to analyze infiltrating cells by flow cytometry. (A-D) Quantification of flow cytometry data showing the percentage (A) and MFI (B) of $CD11c^+$ cells also positive for $MHCII^+$ and the percentage (C) and MFI (D) of $CD11c^+$ cells also positive for $CD86^+$. Representative FACS plots for day 5 shown in Supporting Figure S8. (E) Percentage of $CD11c^+$ cells expressing

negative costimulatory molecules (PD-L1 and PD-L2). (F–G) Flow cytometry plots comparing cell surface marker expression by immature BMDCs *in vitro* (grey) and by cells isolated from gels at day 3 (red, overlaid). (F) Expression of MHCII and CD86. (G) Expression of PD-L1 and PD-L2. (n = 3 per condition per timepoint; mean ± s.d. shown; * $p < 0.05$; *** $p < 0.001$; **** $p < 0.0001$).